Supporting Information for *Acta Phys. -Chim. Sin.* 2017, *33* (5), 993－1000
doi: 10.3866/PKU.WHXB201702087

快速合成廉价 CuMo 纳米粒子高效催化氨硼烷水解产氢

杨 昆[1] 姚淇露[1] 卢章辉[1,*] 康志兵[2] 陈祥树[1,*]

([1]江西师范大学化学化工学院，无机膜材料工程技术研究中心，南昌 330022；
[2]南昌航空大学航天制造工程学院，南昌 330036)

Facile Synthesis of CuMo Nanoparticles as Highly Active and Cost-Effective Catalysts for the Hydrolysis of Ammonia Borane

YANG Kun[1] YAO Qi-Lu[1] LU Zhang-Hui[1,*] KANG Zhi-Bing[2]

CHEN Xiang-Shu[1,*]

([1]*Jiangxi Inorganic Membrane Materials Engineering Research Centre, College of Chemistry and Chemical Engineering, Jiangxi Normal University, Nanchang 330022, P. R. China*; [2]*School of Aeronautical Manufacture Engineering, Nanchang Hangkong University, Nanchang 330036, P. R. China*)

[*]Corresponding authors. LU Zhang-Hui, Email: luzh@jxnu.edu.cn.
CHEN Xiang-Shu, Email: cxs66cn@jxnu.edu.cn..

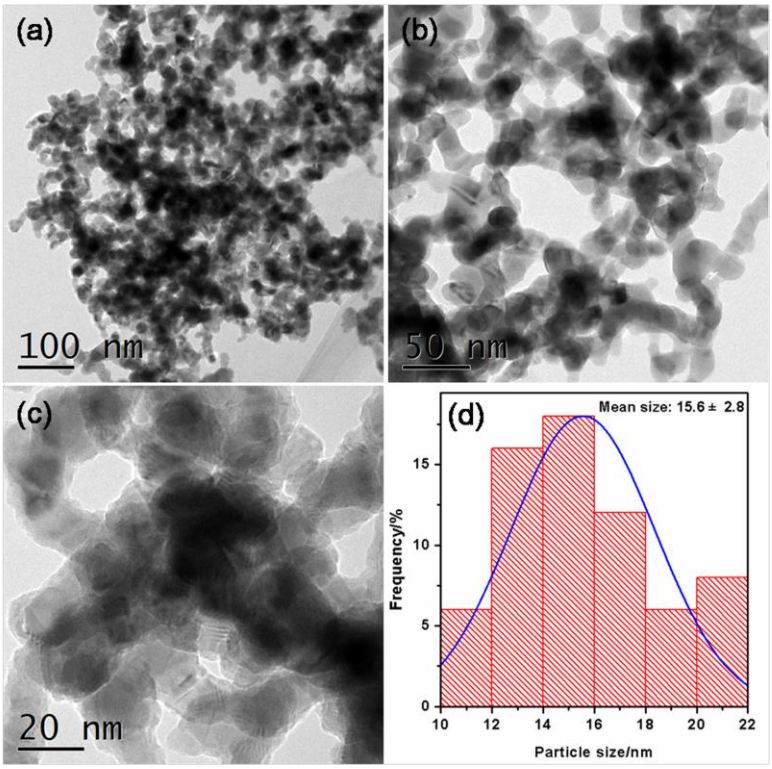

Fig.S1 (a-c) Typical TEM images and (d) size distribution of Cu NPs

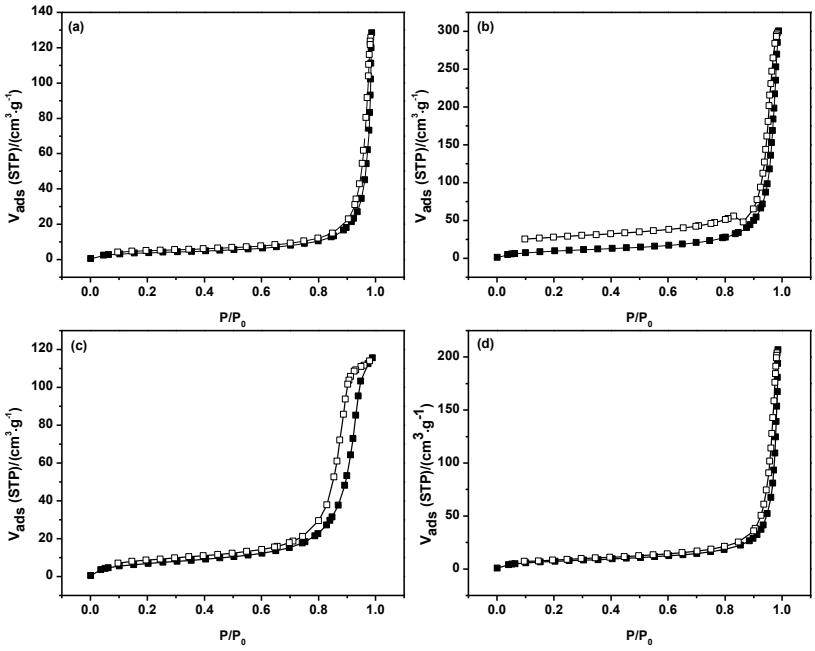

Fig.S2 Nitrogen adsorption-desorption isotherms of the (a) Cu, (b) $Cu_{0.9}Mo_{0.1}$, (c) $Cu_{0.9}W_{0.1}$ and (d) $Cu_{0.95}Cr_{0.05}$ NPs

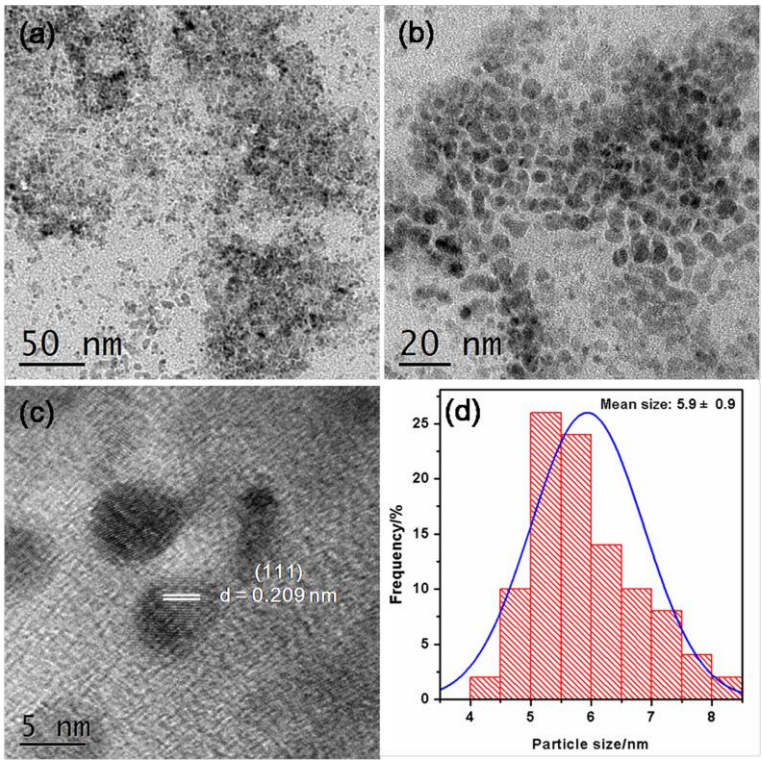

Fig.S3 (a, b) Typical TEM images, (c) high resolution TEM image and (d) size distribution of $Cu_{0.9}W_{0.1}$ NPs

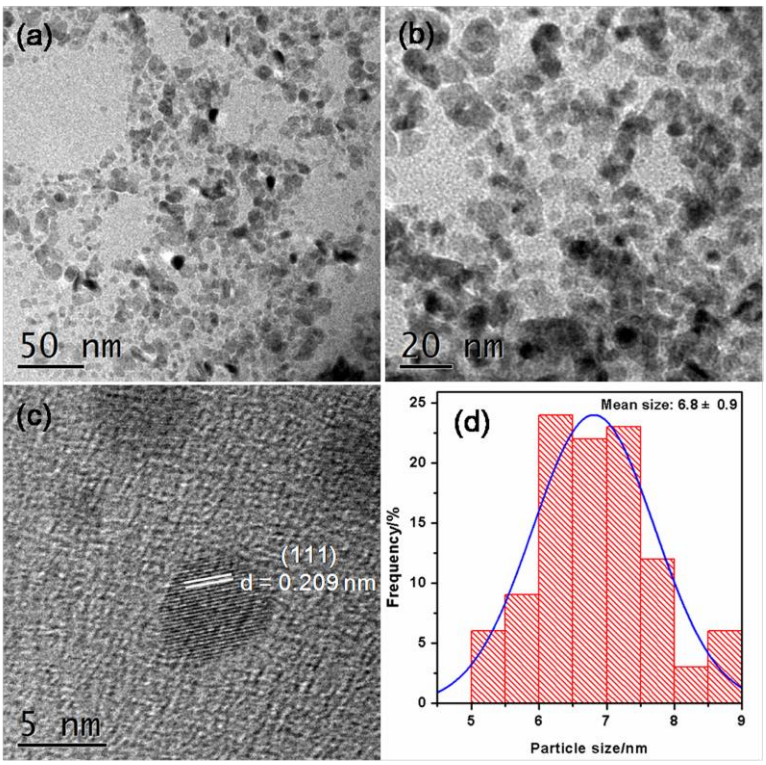

Fig.S4 (a, b) Typical TEM images, (c) high resolution TEM image and (d) size distribution of $Cu_{0.95}Cr_{0.05}$ NPs

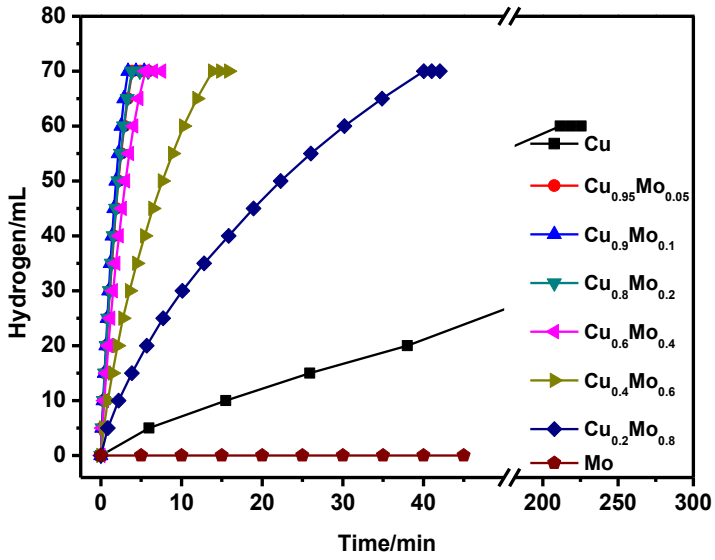

Fig.S5 Hydrogen generation from the hydrolysis of AB (200 mmol·L^{-1}, 5 mL) catalyzed by Cu_xMo_{1-x} NPs with different x value at 298 K (metal/AB = 0.06)

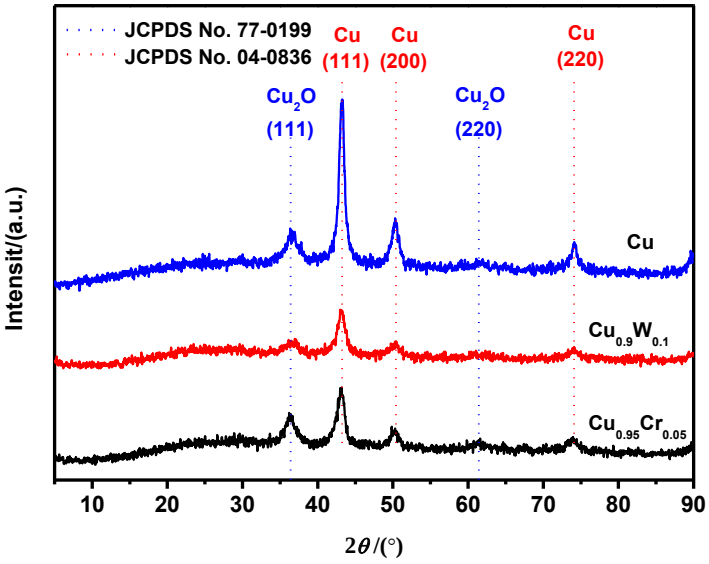

Fig.S6 XRD patterns of Cu, $Cu_{0.9}W_{0.1}$ and $Cu_{0.95}Cr_{0.05}$ NPs

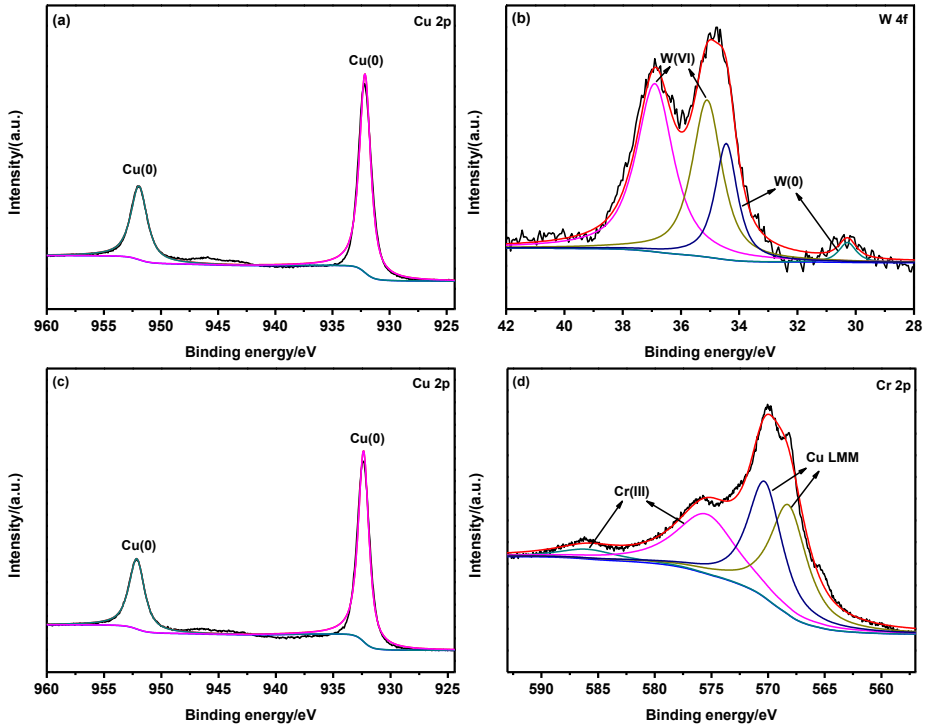

Fig.S7 XPS spectra of (a) Cu 2p and (b) W 4f for the as-synthesized $Cu_{0.9}W_{0.1}$ NPs, (c) Cu 2p and (d) Cr 2p for the as-synthesized $Cu_{0.95}Cr_{0.05}$ NPs after Ar etching

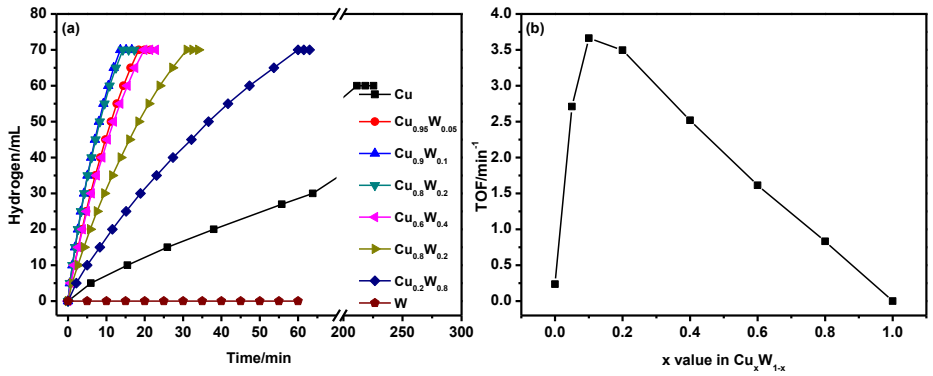

Fig.S8 (a) Hydrogen generation from the hydrolysis of AB (200 mmol·L^{-1}, 5 mL) catalyzed by Cu_xW_{1-x} NPs with different *x* value and (b) the corresponding TOF values for the hydrolysis of AB at 298 K (metal/AB = 0.06)

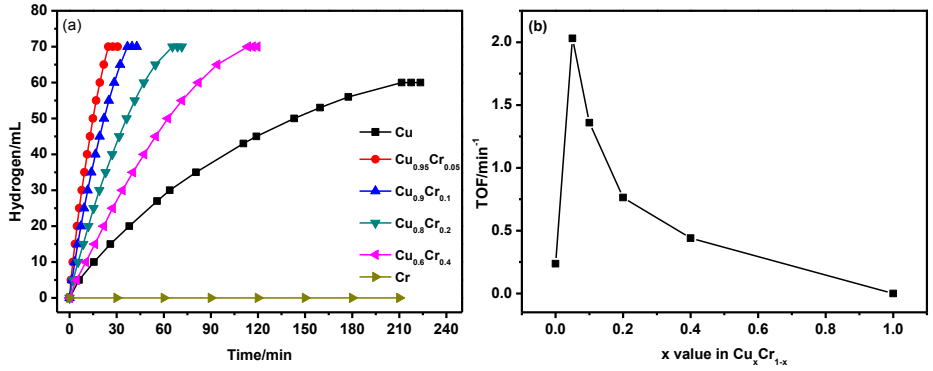

Fig.S9 (a) Hydrogen generation from the hydrolysis of AB (200 mmol·L^{-1}, 5 mL) catalyzed by Cu_xCr_{1-x} NPs with different *x* value and (b) the corresponding TOF values for the hydrolysis of AB at 298 K (metal/AB = 0.06)

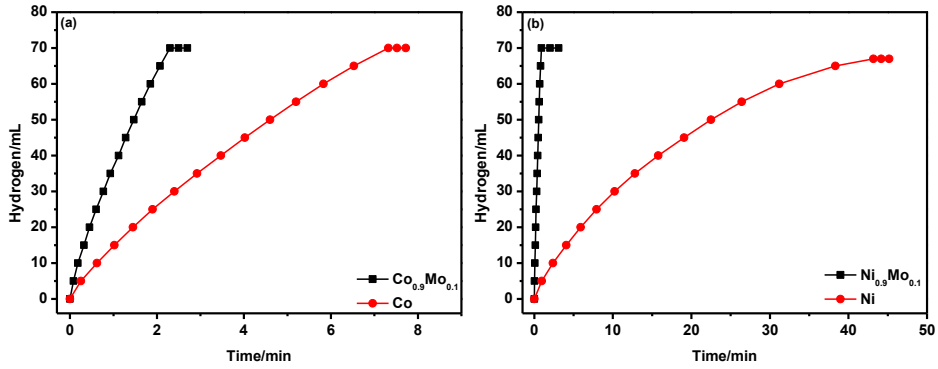

Fig.S10 Hydrogen generation from the hydrolysis of AB (200 mmol·L^{-1}, 5 mL) catalyzed by (a) $Co_{0.9}Mo_{0.1}$, Co NPs and (b) $Ni_{0.9}Mo_{0.1}$, Ni NPs at 298 K (metal/AB = 0.06)

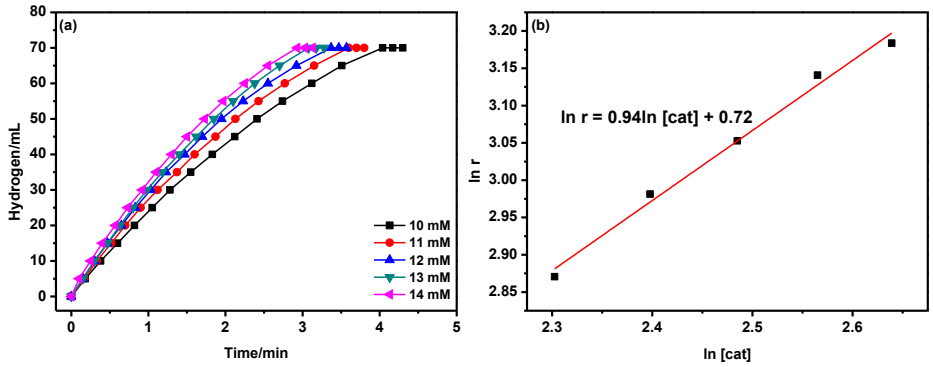

Fig.S11 (a) Hydrogen generation from the hydrolysis of AB (200 mmol·L^{-1}, 5 mL) catalyzed by $Cu_{0.9}Mo_{0.1}$ NPs with different catalyst concentrations at 298 K and (b) ln[cat] *vs* ln*r* plot

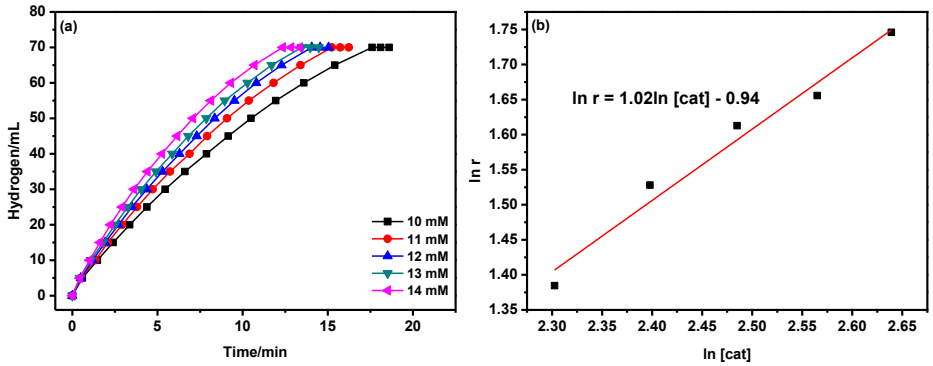

Fig.S12 (a) Hydrogen generation from the hydrolysis of AB (200 mmol·L^{-1}, 5 mL) catalyzed by $Cu_{0.9}W_{0.1}$ NPs with different catalyst concentrations at 298 K and (b) ln [cat] *vs* ln*r* plot

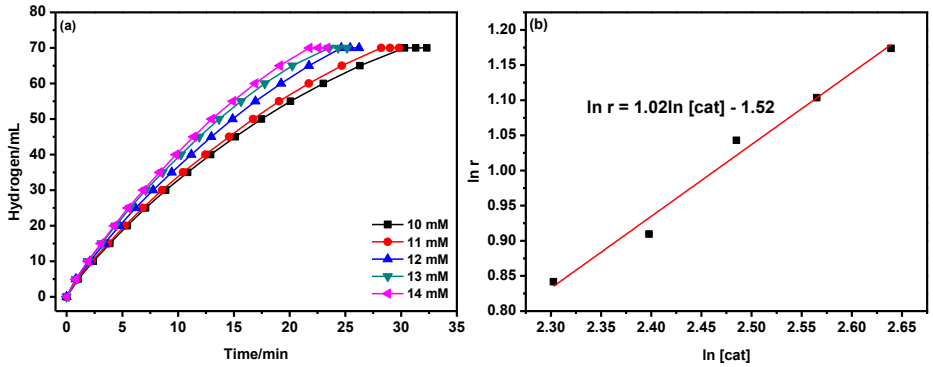

Fig.S13 (a) Hydrogen generation from the hydrolysis of AB (200 mmol·L^{-1}, 5 mL) catalyzed by $Cu_{0.95}Cr_{0.05}$ NPs with different catalyst concentrations at 298 K and (b) ln[cat] *vs* ln*r* plot

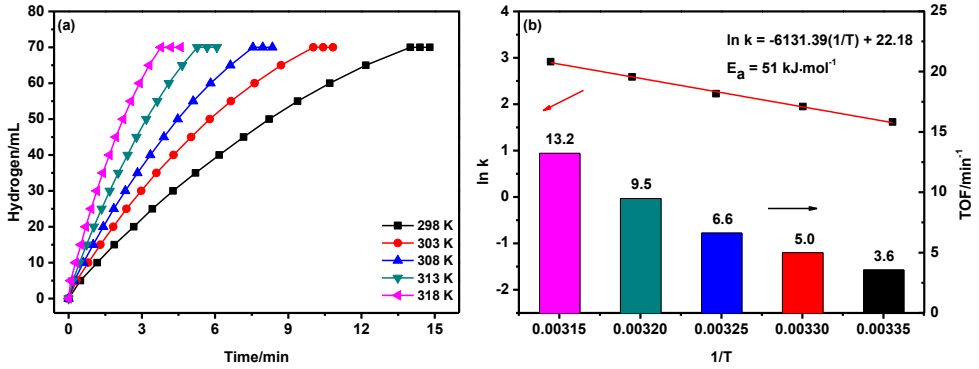

Fig.S14 (a) Hydrogen generation from the hydrolysis of AB (200 mmol·L^{-1}, 5 mL) and (b) Arrhenius plots and TOF values of AB hydrolytic dehydrogenation catalyzed by $Cu_{0.9}W_{0.1}$ NPs at different temperatures (metal/AB = 0.06)

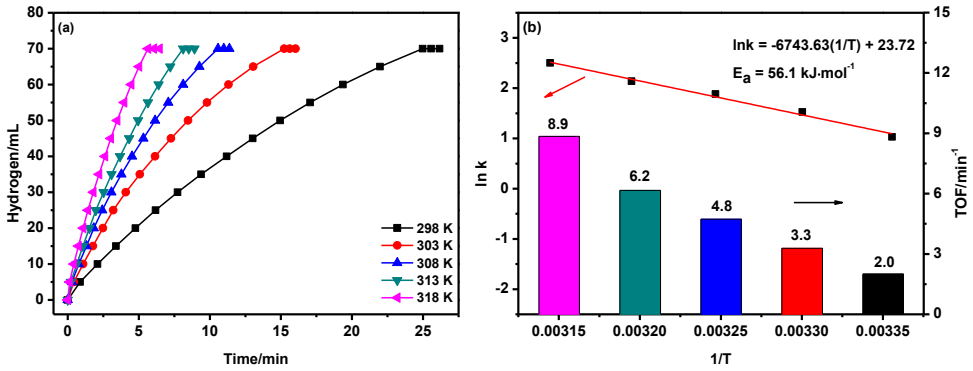

Fig.S15 (a) Hydrogen generation from the hydrolysis of AB (200 mmol·L^{-1}, 5 mL) and (b) Arrhenius plots and TOF values of AB hydrolytic dehydrogenation catalyzed by $Cu_{0.95}Cr_{0.05}$ NPs at different temperatures (metal/AB = 0.06)

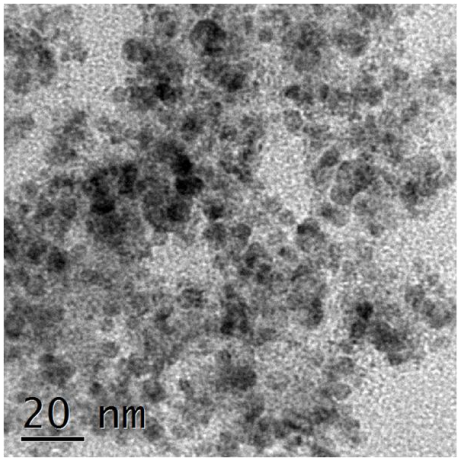

Fig.S16 TEM image of $Cu_{0.9}Mo_{0.1}$ NPs after the 5th catalytic reuse